

UC Berkeley

Controls and Information Technology

Title

Evaluation of various CFD modelling strategies in predicting airflow and temperature in a naturally ventilated double skin facade

Permalink

<https://escholarship.org/uc/item/9r65g9k7>

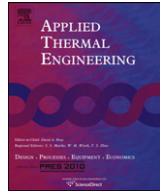
Authors

Pasut, Wilmer
De Carli, Michele

Publication Date

2011-11-01

Peer reviewed



Evaluation of various CFD modelling strategies in predicting airflow and temperature in a naturally ventilated double skin façade

Wilmer Pasut ^{a,*}, Michele De Carli ^b

^a University of California at Berkeley, Center for the Built Environment 390 Wurster Hall #1839, Berkeley, CA 94720-1839, USA

^b Dipartimento di Fisica Tecnica, Università degli Studi di Padova, Via Venezia 1, 35131 Padova, Italy

ARTICLE INFO

Article history:

Received 8 December 2009

Accepted 14 November 2011

Available online 22 November 2011

Keywords:

Double skin façade

CFD

Natural ventilation

Performance simulation

Thermal performance

Air flow

ABSTRACT

Demands for energy savings, thermal and visual comfort and a high-tech image for new building envelopes can be met with a Double Skin Façade (DSF). These kinds of building envelopes are widely encouraged, proposed and increasingly designed by architects. Naturally ventilated DSFs seem very interesting from an energy point of view, but a good design is crucial to improve the energy savings and the proper operation of the system. Computational Fluid Dynamics (CFD) can play an important role in evaluating and improving the thermal behaviour of a DSF. This paper shows, through a sensitivity analysis, a good strategy for carrying out a CFD simulation of this special building envelope. In this work the validations of the results are based on experimental data from the literature.

The paper provides a discussion that highlights which factors are important in the simulation, and which increase model complexity without improving the prediction capacity. The results show that, for a DSF characterized by a prevalent bidirectional flow, the additional effort required to make a 3D model is not justified by a significant improvement of the results. This work shows also that the accuracy can be improved by modelling outdoor ambient. The performance of $k-\epsilon$ and $k-\omega$, the two most commonly used turbulent models for simulating the naturally ventilated DSF is evaluated.

© 2011 Elsevier Ltd. All rights reserved.

1. Introduction

In the last years, new building envelope systems have been developed in order to improve thermal insulation, to shade solar radiation and to provide suitable thermal and visual comfort conditions. One of these special types of envelopes is “Double Skin Façade” (DSF). DSF are made with two layers of glass separated by a significant amount of air space. The space between the glasses can be ventilated with three different strategies: mechanical ventilation, natural ventilation or hybrid. The ventilation of the air gap contributes to saving energy both during the summer and the winter time. In fact, during the winter time, the air between the glass is heated by the sun rays (greenhouse effect [1]), thus improving the thermal performance of the façade with a consequent reduction of heating costs. With hybrid ventilation systems, during the winter, the fresh air can be pre-heated in the DSF gap before entering in the HVAC system. During the summer, the air flow through the DSF (mechanical or natural) can help to decrease the temperature in the gap.

A blind for solar control is usually installed in the DSF gap. In addition to reducing heat gain during the summer, this blind increases airflow through the gap with a strong buoyancy effect. In mild seasons, stack effect occurring in the intermediate space can be used as driving force to promote natural ventilation of the whole building [2].

The correct behaviour of a DSF is the key to increasing energy savings, but correct behaviour requires the structure to be designed correctly. One of the weakest spots of this kind of envelope is the design, especially for naturally ventilated façades, where the thermal process and the airflow mechanism influence each other. The magnitude and extent of this interaction depend on the geometric features of system, and the thermal and optical properties of various components.

Ventilated facades are already a common feature of architectural competitions in Europe; but there are still relatively few buildings in which they have actually been realized, and there is still too little experience of their behaviour in operation [1,3,4]. For this reason the CFD analysis could be one of the most important tools to predict the behaviour of DSF and help architects make decisions during the design process.

In the literature there are several examples of using CFD to study the behaviour, features and energy consumption of a DSF [5–7].

* Corresponding author. Tel.: +1 510 642 4950; fax: +1 510 643 5571.

E-mail addresses: wpasut@berkeley.edu, wilmer.pasut@gmail.com (W. Pasut).

The advances in computing power and commercial CFD software available to building mechanical engineers make it possible to use this tool [8]. Using CFD does not necessarily ensure accurate results [9] and it requires engineering judgment [8,10]. Thus the steps of validation, verification, and reporting results described by Chen and Srebric [8] are of great importance.

This research discusses the primary parameters that can influence CFD results during a modelization of natural ventilated DSF. This was carried out through an accurate sensitivity analysis.

The model was compared by using Mei' measurements [11]. These measures were used for two reasons:

- they were carried out in a laboratory, so they were not influenced by wind. The instability of wind can strongly influence the DSF behaviour and make the comparison between CFD and experimental results problematic;
- the velocity and temperature fields inside the gap are presented in the Mei' paper. These can be compared with the CFD velocity and thermal fields to better understand the impact of a different user's choices;

The key points of a sensitive analysis are:

- air property definitions, as constants or as a function of temperature;
- turbulence model;
- presence or absence of external environment;
- 2D or 3D model.

The scope of this work is to show the effects that principal simulation parameters have on CFD results. The scope was not to validate the model. This is because of the other actions, like modifying the CFD model dimensions [5], were not performed in order to improve the results agreement.

The model was realized with the commercial software Fluent [15]. Fluent was used in other similar works [10] [6].

2. Case description

In this work a typical single-story commercial façade was modeled. The main dimensions of a double skin were drawn from an article by Mei [11]. The CFD model was realized with the following dimensions: the outer skin of the façade is a single 12 mm thick clear glass pane, which is 144 cm wide and 206 cm high comprising an aluminium frame. The glass area is 128 cm wide and 191 cm high. In the Mei' case study both the air intake and exhaust of the DSF are designed as a commercial grille arrangement to permit air flow through the façade cavity. The grilles are 24 cm high and 145 cm wide. Each grille has three 4.5 cm high spaces for air ingress and egress. The inner skin is 138 cm × 200 cm and the glass area is 122 cm × 185 cm. The sun-shading blind is a venetian type blind. The blind is made of aluminium and is 2.1 m high and 1.45 m wide. The blades are 8 cm wide and the blade angle is 45°. The cavity of air is 55 cm wide and the blind is located at one third of the cavity width as measured from the outer skin [11]. With these dimensions the CFD model was realised. The Mei' test was carried out with fixed values for radiance, inner temperature, and outer temperature. The values for those three parameters are 715 Wm⁻² for the irradiance (used as a benchmark) and 20 °C for both "indoor" and "outdoor" temperature.

3. Boundary conditions and numerical methods

The inside air temperature (temperature inside the room) was the same as outside, 293.15 K. The air ingress and egress are

modelled as a pressure inlet and pressure outlet with the same gauge total pressure equal to 0. In Fig. 1 a simplified section of the double skin is shown.

The solar radiation was not directly simulated but the surface temperatures measured by Mai et al. were used as boundary conditions. This was advantageous considering the next step of this work, coupling of CFD program with the energy simulation program "EnergyPlus" [12]. The method of combining CFD and ES program will be the Virtual Dynamic Coupling (as proposed by Chen and Van Der Kooi [13], and [14]), where temperatures are one of the information exchanged between the two software.

The air density was defined as a polynomial function of temperature as follows,

$$\rho = 3.34697 - 0.01055708 \cdot T + 1.10772e^{-5} \cdot T^2 \quad (1)$$

For this function the program Refprop 7 has been used.

The simulations used the first-order upwind scheme for all of the variables except pressure. The pressure discretization used the Body-Force Weighted scheme [15]. The SIMPLE algorithm was adopted to couple the pressure and the momentum equations. Usually if the sum of absolute normalized residuals for all of the cells in the domain became less than 10⁻⁶ for energy and 10⁻³ for other variables, the solution was considered converged [16], but the simulations show that the velocity and temperature fields still changed after convergence. For this reason, to be sure the results were stable, the number of iterations was doubled.

3.1. Mesh features

The mesh and the relative number of cells is a critical parameter that strongly influences the computational time. Increasing the number of cells can often increase computational time by an order of magnitude. Furthermore, the grid dimensions influence the accuracy of CFD results and the value of y^+ . The parameter y^+ is critical to the correct use of turbulence models. Before doing the simulations different meshes were tested, for 2D and 3D models, in order to figure out the minimum amount of cells that can guarantee the invariability of the results. An important feature of the mesh is that the y^+ value must be less than, or close to, 1 for the first grid close to the walls. That has permitted the use of $k-\epsilon$ with enhanced wall treatment, and $k-\omega$ models as turbulent models.

In the 2D models the mesh used has:

- 436 000 nonuniform cells. The corresponding y^+ was about 0.6 for the first grid close to the walls, and the computational time was 7 s per iteration

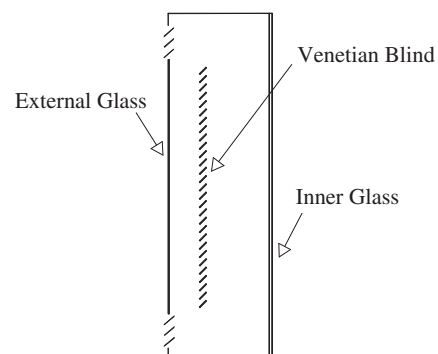


Fig. 1. Section of double skin façade.

The 3D models:

- 1 930 000 nonuniform cells. The computational time was 45 s per iteration. The y^+ value was close to 1;

One important thing requires explanation. Firstly in order to better understand the time per iteration, it is important know that the simulations were conducted on a personal computer with a Core2 2.0 GHz CPU and 2 GB memory.

4. Sensitivity analysis

An accurate sensitivity analysis was carried out for every parameter that could influence the quality of the results. In this section the different parameters are discussed separately.

4.1. Air properties

The existence of gravity and fluid density differentials cause the buoyancy effects that move the air through the gap. The thermal plumes are generated by the temperature difference between the surfaces and the air. The temperature therefore influences the air density as well as influences other air properties such as thermal conductivity λ [$\text{W m}^{-1} \text{K}^{-1}$] and c_p [$\text{J kg}^{-1} \text{K}^{-1}$]. The simulations can be carried out with keeping the air properties λ and c_p as constant values or considering as polynomial functions of temperature. It is interesting to estimate how much the difference is between treating these two parameters as constants and as functions of T . The estimation can be done even without comparing the results of two different CFD simulations, because the highest temperature gradient in the DSF can be easily estimated. The following polynomial functions were deduced with the program Refprop 7:

$$\lambda = -0.43373e^{-3} + 0.11699e^{-3} \cdot T - 0.12e^{-6} \cdot T^2 \left[\text{Wm}^{-1} \text{K}^{-1} \right] \quad R^2 = 1 \quad (2)$$

$$c_p = 1032.28915 - 0.20724 \cdot T + 0.40574e^{-3} \cdot T^2 \left[\text{Wm}^{-1} \text{K}^{-1} \right] \quad R^2 = 0.998 \quad (3)$$

The constant values for the same property were expressed for the reference temperature $T = 293.14$ [K]:

$$\lambda = 0.23549e^{-1} \left[\text{Wm}^{-1} \text{K}^{-1} \right] \quad (4)$$

$$c_p = 1006.4 \left[\text{Jkg}^{-1} \text{K}^{-1} \right] \quad (5)$$

The lower temperature in the model is the air temperature ($T_{\text{air}} = 293.15$), while the higher temperature is the external glass temperature ($T_{\text{ex,gl}} = 317.15$). The max value for the thermal gradient can be easily estimated. It is the difference between T_{air} and $T_{\text{ex,gl}}$, which is $\Delta T = 22$. It means that λ maximum variation due to the temperature gradient inside the DSF is $\Delta \lambda = 0.00105$ [$\text{W m}^{-1} \text{K}^{-1}$]. It is 2.6% of the λ value at 293.15 K. For the c_p value the variation due to the ΔT is 1 [$\text{J kg}^{-1} \text{K}^{-1}$], which means it is less than 0.1% of the c_p value at 293.15 K. These results easily demonstrate that considering the λ and c_p values as functions of temperature is not worthy, since it only increases the execution time without significant improvement of the CFD prediction.

4.2. Turbulence model

Proper selection of a turbulence modelling method is of great importance to accuracy and efficiency of the model. Thus it is

important to conduct a sensitivity analysis for the two of most popular turbulence model as well are used:

- k- ω SST;
- k- ϵ RNG with enhanced wall function.

As presented in the Table 1, which is an excerpt from Zhang Z. et al. [16], both models predict mean temperature and mean velocity well in the presence of natural convection. The ratings in Table 1 were deduced for an internal environment, but the results are still valid for this work because the Mei' experiments are carried out in an internal environment without wind.

Both k- ϵ and k- ω are RANS turbulence eddy-viscosity models, and they belong to the subcategory called Two-Equations. They use the same equation for the turbulent kinetic energy k [17]:

$$k = \frac{1}{2} u_i' u_i' \quad (6)$$

but a different equation for rate of energy kinetic dissipation:

$$\epsilon = k^{3/2} / l \quad [18] \quad (7)$$

$$\omega = k^{3/2} / l \quad [19] \quad (8)$$

The equation for turbulent eddy viscosity is also different:

$$\mu_t = \rho C_\mu \frac{k^2}{\epsilon} \quad \text{for the k - } \epsilon \text{ model} \quad (9)$$

where C_μ is a constant equal to 0.09 for standard k- ϵ or 0.0845 per k- ϵ RNG.

$$\mu_t = \rho \alpha^* \frac{k}{\omega} \quad \text{for the k - } \omega \text{ model} \quad (10)$$

where the coefficient α^* damps the turbulent viscosity causing a low-Reynolds-number correction [15]. The μ_t equation for SST is more complicated; more details on this aspect could be found in to Fluent User's Guide [15].

The RNG k- ϵ model is similar in form to the standard k- ϵ model, but includes the following refinements [15]:

- The RNG model has an additional term in its ϵ equation that significantly improves the accuracy for rapidly strained flows.
- The effect of swirl on turbulence is included in the RNG model, enhancing accuracy for swirling flows.
- The RNG theory provides an analytical formula for turbulent Prandtl numbers, while the standard k- ϵ model uses user-specified, constant values.
- While the standard k- ϵ model is a high-Reynolds-number model, the RNG theory provides an analytically-derived differential formula for effective viscosity that accounts for low-Reynolds number effects. Effective use of this feature does, however, depend on an appropriate treatment of the near-wall region.

Table 1

Excerpt from Zhang Z. et al [16] for the results in the case of natural convection in a room.

Natural convection	Compared items	Turbulence models	
		k- ϵ RNG	k- ω SST
	Mean temp.	A	A
	Mean velocity	B	A
	Turbulence	C	C

A = good, B = acceptable, C = marginal, D = poor.

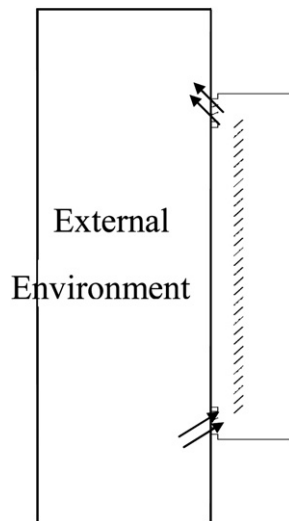


Fig. 2. Scheme of the CFD model used with the external environment.

The last point is the reason the Enhanced Wall Treatment was adopted for the RNG $k-\epsilon$ model. During the simulations, the Full Buoyancy Effects option was turned on [15].

The SST $k-\omega$ model is similar to the standard $k-\omega$ model, but includes the following refinements:

- The standard $k-\omega$ model and the transformed $k-\epsilon$ model are both multiplied by a blending function and added together. The blending function is designed to be one in the near-wall region, which activates the standard $k-\omega$ model, and zero away from the surface, which activates the transformed $k-\epsilon$ model.
- The SST model incorporates a damped cross-diffusion derivative term in the ω equation.
- The definition of the turbulent viscosity is modified to account for the transport of the turbulent shear stress.
- The modelling constants are different.

4.3. External environment

The presence or absence of external environment is another key point investigated in this paper. In fact without the modelization of

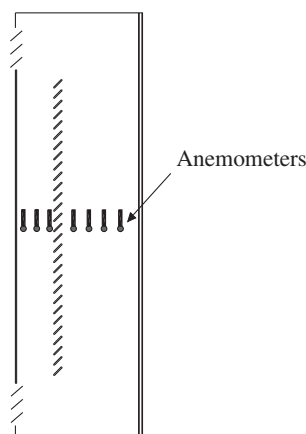


Fig. 3. Anemometers positions in the measurement work.

Table 2
Ratings for air velocity prediction.

Simulation features	Points						
	1	2	3	4	5	6	7
1 2D, $k-\omega$ SST	C	B	D	C	A	C	D
2 2D, $k-\epsilon$ RNG	C	B	C	D	A	C	C
3 2D, $k-\omega$ SST, with external environ.	C	C	D	D	C	C	A
4 2D, $k-\epsilon$ RNG, with external environ.	C	B	C	D	A	B	B
5 3D, $k-\omega$ SST	B	A	C	C	C	B	D
6 3D, $k-\epsilon$ RNG	C	A	B	D	B	B	C
7 3D, $k-\omega$ SST, with external environ.	B	A	D	C	D	B	D
8 3D, $k-\epsilon$ RNG, with external environ.	B	A	B	C	B	B	C

an ambient air close to the ingress and egress of a DSF, the user must specify the air direction of the pressure inlet, and the air direction and temperature of the backflow air in the pressure outlet. Fig. 2 shows the CFD model with external environment. Its dimensions are 3.8 m high by 1.2 m wide. The air direction for the pressure inlet in the model without external environment, can be left "Normal to Boundary", which is the default setting, but in order to improve the result quality an angle same as the ingress grill angle was used for the air direction in the ingress boundary condition.

4.4. 2D or 3D model

The airflow pattern in the core region of a DSF is almost bi-directional, but is the third direction negligible in comparison with the other two? This was true in the Betts and Bokhari experimental investigation of natural convection in a tall cavity [20], but what this work has investigated is if the effects of third direction are negligible also during the modelization of a natural ventilated DSF.

5. Results

The predicted results were compared with the experimental data. The model accuracy criteria used to evaluate the difference between experimental data and CFD results are quite similar to that used by Zhang et al. [16]. This model quantifies the relative error between prediction and measured points. If this error is less than 10% the rating is A, between 10% and 30% the rating is B, from 30% to 50% is C, while greater than 50% the rating is D. The scale was improved in order to evaluate temperature results, because there were a lot of points in the error range from 10% to 30%. To improve the results' legibility, the B+ rating was added. This rating is assigned for errors between 10% and 20%. For errors between 20% and 30%, the B rating was still used.

The experimental data were collected in the core of the DSF with seven omni-directional anemometers, these were arranged along

Table 3
Ratings for temperature prediction.

Simulation features	Points						
	1	2	3	4	5	6	7
1 2D, $k-\omega$ SST	C	C	C	C	B	C	B
2 2D, $k-\epsilon$ RNG	B	B	B	B	B	C	B
3 2D, $k-\omega$ SST, with external environment	B	B+	B+	B+	B+	B	B+
4 2D, $k-\epsilon$ RNG, with external environment	B	B+	B	B	B+	B	B+
5 3D, $k-\omega$ SST	B	B	B	B	B	B	B
6 3D, $k-\epsilon$ RNG	B	B	B	B	B	C	B
7 3D, $k-\omega$ SST, with external environment	B	B+	B	B	B	C	B
8 3D, $k-\epsilon$ RNG, with external environment	B	B	B	B	B	B	B

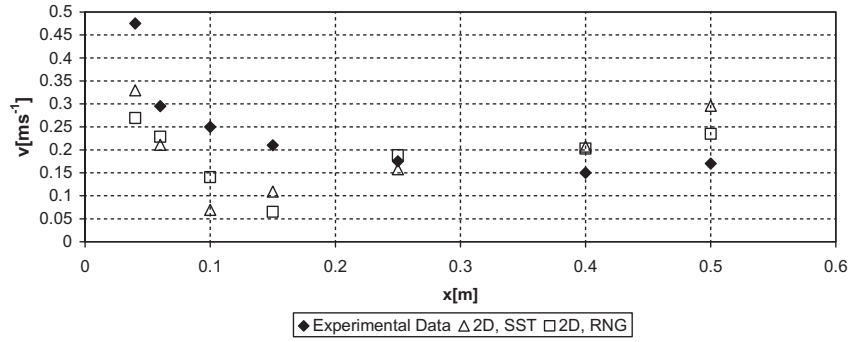


Fig. 4. Comparison on air velocity between experimental results and simulations 1 and 2.

a line from the inner glass to the outer glass, as Fig. 3 shows. The CFD data have been collected in the same positions.

Tables 2 and 3 show the ratings for velocity field and thermal field respectively. The ratings are presented for every point. The

points are enumerated from the inner glass to the outer glass. Figs 4–7 show the results compared with each other and with the experimental data for velocity field. Figs 8–11 show the results for air temperatures.

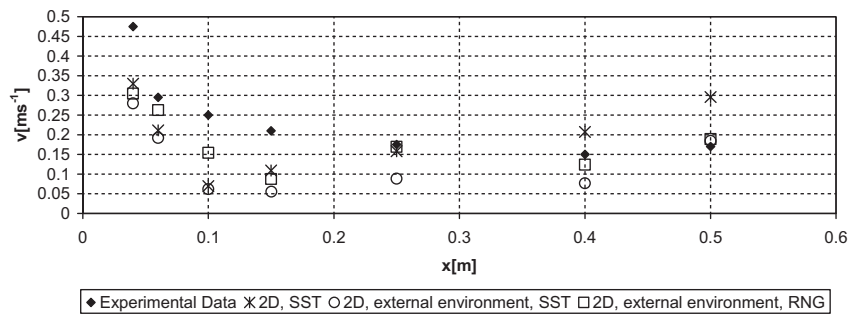


Fig. 5. Comparison on air velocity between experimental results and simulations 1, 3, and 4.

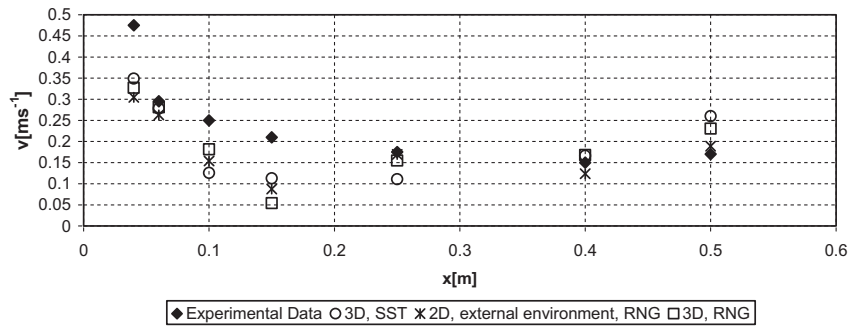


Fig. 6. Comparison on air velocity between experimental results and simulations 4, 5, and 6.

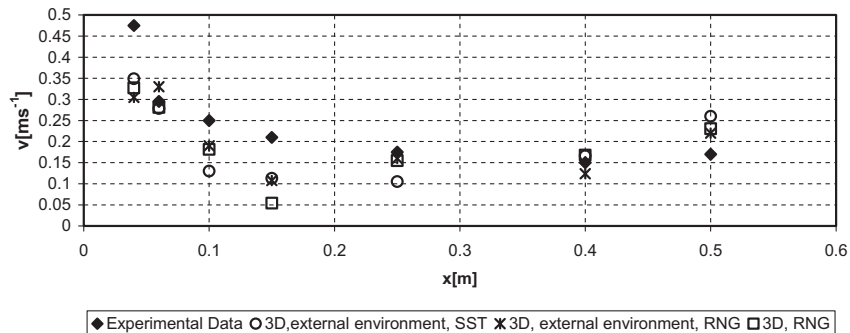


Fig. 7. Comparison on air velocity between experimental results and simulations 6, 7, and 8.

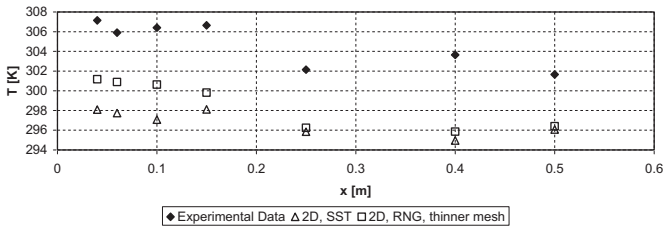


Fig. 8. Comparison on temperature between experimental results and simulations 1 and 2.

Figs. 12 and 13 represent respectively the velocity field in the double skin façade and the path line. As it can be seen from the two figures that the cool air enters from the bottom inlet and slowly rises into the gap moving from the inner glass to the external glass. This phenomena can explain why the temperature measured on the right side of the gap are always lower than the temperatures measured on the left side of the gap.

From the detail of the velocity field close to the blind in Fig. 14, it can be seen that the air velocity through the blind is very slow and no eddy is generated before and after the blind where the anemometers are located.

For sake of completeness in Fig. 15 the temperature field into the double skin façade is presented.

6. Discussion

The velocity field prediction is slightly improved by the addition of external environment in the case using the RNG turbulent model. In the case using the SST model, adding the external environment worsens the prediction for two points and improves it only for one. The thermal field prediction is noticeably improved in both cases. For both cases the presence of external environment improves the velocity prediction in the DSF part between the venetian blind and the inner glass. More than 60% of the total air flowing inside the DSF passes through this region. Thus improving the prediction of this part gives better prediction in the entire DSF.

Switching from a 2D model to a 3D does not show an appreciable difference in the results. It means that it is not worthy to make a 3D model in case of DSF. The results of a 2D model are almost as those of a 3D model even with a remarkable computational time saving.

Looking at the prediction results for point four in Table 2, almost every simulation presents an unacceptable error for that point. One likely reason for this is the slight differences between real case and

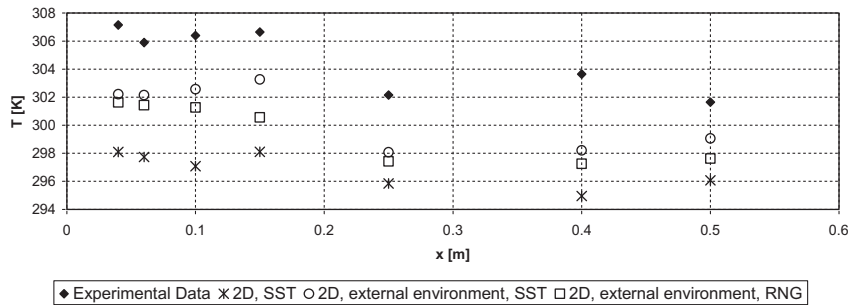


Fig. 9. Comparison on temperature between experimental results and simulations 1, 3, and 4.

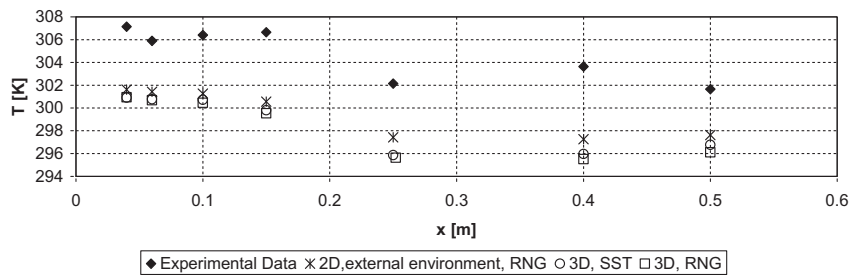


Fig. 10. Comparison on temperature between experimental results and simulations 4, 5, and 6.

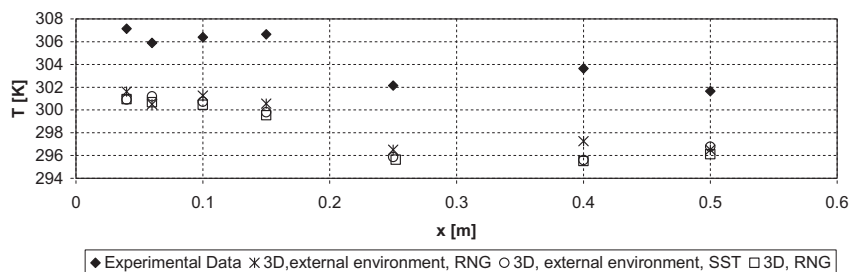


Fig. 11. Comparison on temperature between experimental results and simulations 6, 7, and 8.

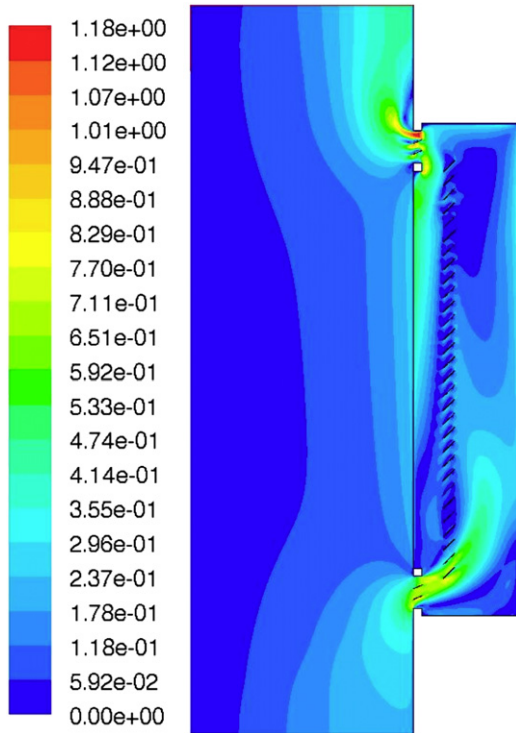


Fig. 12. Predicted velocity [ms^{-1}] field in the double skin façade.

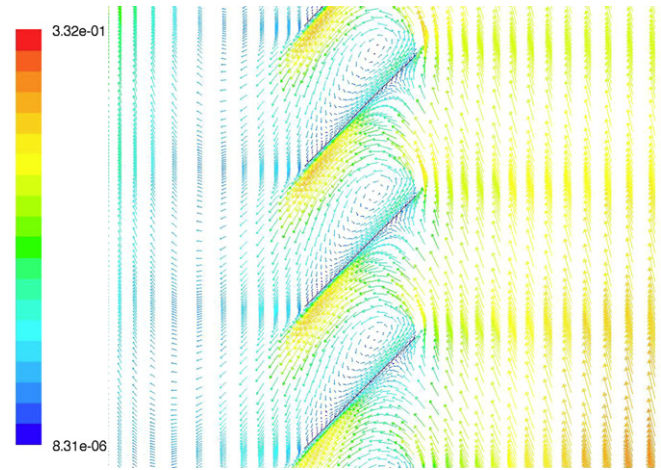


Fig. 14. Particular of velocity [ms^{-1}] field close to the central blind.

model dimensions. In fact, the air flow comes through the venetian blind from the inner part of DSF to the outer part, and point four is the closest to the blind. It means that if the air velocity is measured 1 cm higher or lower, the value can change greatly.

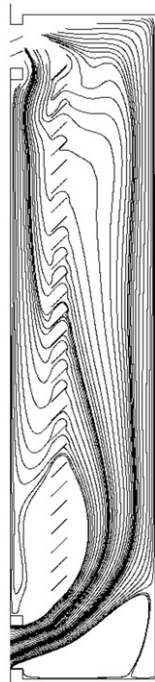


Fig. 13. Path lines inside the double skin façade.

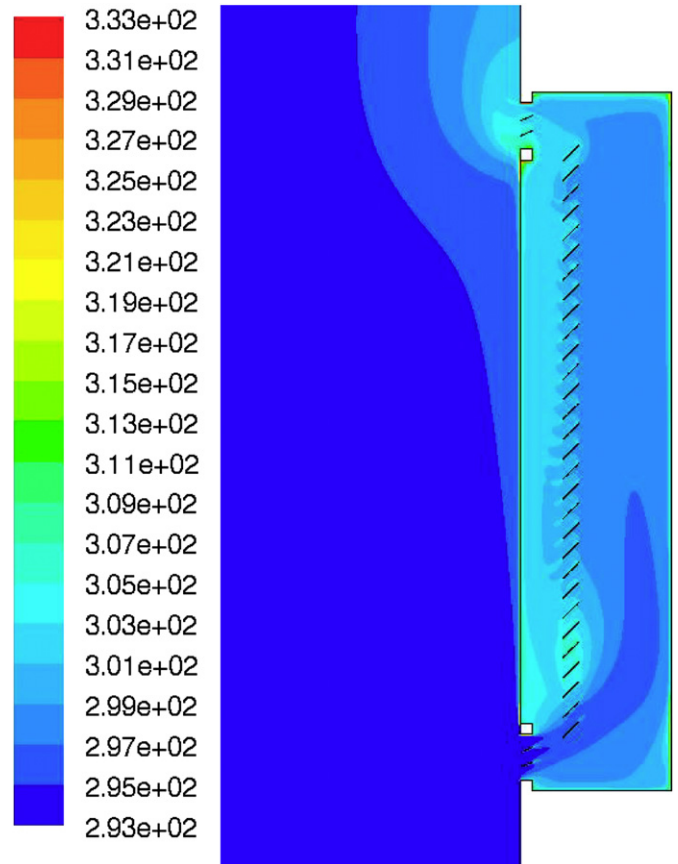


Fig. 15. Temperature [K] field in the double skin façade.

7. Conclusions

A CFD model for the natural ventilated double skin façade was developed. The model can be used to predict the airflow patterns, air temperature and air velocity distributions, and heat flux from gap into the room. The model was validated using experimental data collected in a full-scale double skin module test facility by Mai et al. The computed air temperature, and velocity generally agree well with the measured data. Furthermore the simulation results show some interesting aspects:

- in the natural ventilated DSF the velocity field is almost bidirectional. This is the reason the 2D CFD model gives the same or better results compared to a 3D model. It means that to study this kind of DSF, a 2D model is the best choice because it guarantees a good prediction with less time demand;
- the results are better for the models with $k-\epsilon$ RNG as a turbulent model. Therefore the $k-\epsilon$ RNG model is advisable for good results and also for good simulation stability;
- the external environment modelization is important for the simulation quality. An adequate ambient air frees the user from deciding the air inlet direction and makes this more reliable.

For the simulations the buoyancy force has to be underlined, as it shows strong influence during the simulations. When the Boussinesq approximation is not used (it can be used only for quite small ΔT), the term ρ_0 appears in the body-force term in the momentum equations as $(\rho - \rho_0) g$ [15]. The term ρ_0 is called the *Operating Density* and it is defined by the CFD user. If it is not, the CFD program uses the average density value calculated in the whole domain as Operating Density. Defining the body-force in this way is slightly detrimental for the prediction results. Setting the body-force for every cell to a constant value instead of using the air-density of neighboring cells causes different local behaviour for every element. This has repercussions on the entire velocity field. The simulations show that if no value is specified, the flow field is erroneous. The reason is the average density is higher than the density of air has at 293.15 K (outer temperature) this causes a reverse flow for a big part of DSF. This is much more evident in simulations where temperature differences are higher. Reasonable results were collected with an Operation Density for the air at 293.15 K (this was the value for the simulations), but an approximation still influences the results.

More experimental work has still to be done in order to check the validity of models with respect of other operating conditions, i.e. different outside air temperatures as well as different values of solar radiation.

Nomenclature

$u_{i,j,k}$	components of the velocity according to i, j, k [m s^{-1}]
ρ	air density [kg m^{-3}]
μ_t	turbulent viscosity [$\text{kg m}^{-1} \text{s}^{-1}$]
k	turbulent kinetic energy
C_μ	empirical constant in the $k-\epsilon$ equations
ϵ	turbulence dissipation rate
ω	specific dissipation rate
α^*	this coefficient damps the turbulent viscosity causing a low-Reynolds-number correction

l	length scale
T	temperature [K]
R^2	coefficient of determination

References

- [1] E. Gratia, A. De Herde, Greenhouse effect in double-skin façade, *Energy and Buildings* 39 (2007) 199–211.
- [2] G. Ballestini, M. De Carli, N. Masiero, G. Tombola, Possibilities and limitations of natural ventilation in restored industrial archaeology buildings with a double-skin façade in mediterranean climates, *Building and Environment* 40 (2005) 983–995.
- [3] A. Zöllner, E.R.F. Winter, R. Viskanta, Experimental studies of combined heat transfer in turbulent mixed convection fluid flows in double-skin-facades, *International Journal of Heat and Mass Transfer* 45 (2002) 4401–4408.
- [4] T. Pasquay, Natural Ventilation in High-rise Buildings with Double Facades, Saving or Waste of Energy. 18th International Conference on Passive and Low Energy Architecture, Brazil, 2001.
- [5] A. Pappas, Z. Zhai, Numerical investigation on thermal performance and correlations of double skin façade with buoyancy-driven airflow, *Energy and Buildings* 40 (2008) 466–475.
- [6] N. Safer, M. Woloszyn, J.J. Roux, Three-dimensional simulation with a CFD tool of the airflow phenomena in single floor double-skin façade equipped with a venetian blind, *Solar Energy* 79 (2005) 193–203.
- [7] P. Ye, S.J. Harrison, P.H. Oosthuizen, Convective heat transfer from a window with a venetian blind: detailed modeling, *ASHRAE Transactions* (1999) 1031–1037.
- [8] Q. Chen, J. Srebric, A procedure for verification, validation, and reporting of indoor environment CFD analyses, *HVAC&R Research* 8 (2002) 201–216.
- [9] Q. Chen, Computational fluid dynamics for HVAC-successes and failures, *ASHRAE Transactions* 103 (1997) 178–187.
- [10] N.M. Post, Airflow models gaining clout, *ENR* 233 (1994) 1311–1332.
- [11] L. Mei, D.L. Loveday, D.G. Infield, V. Hanby, M. Cook, Y. Li, M. Holmes, J. Bates, The influence of blinds on temperatures and air flows within ventilated double-skin façades. Proceedings of clima 2007 WellBeing Indoors, (http://usir.salford.ac.uk/15870/1/Clima_2007_B02E1606.pdf).
- [12] EnergyPlus Input Output Reference, The Encyclopedic Reference to EnergyPlus Input and Output (2010). <http://www.energyplus.gov> [Online].
- [13] Q. Chen, J. van der Kooij, A computer program for combined problems of energy analysis, indoor airflow, and air quality, *ASHRAE Transaction* 94 (2) (1988) 196–214.
- [14] Z. Zhai, Q. Chen, P. Haves, J.H. Klems, On approaches to couple energy simulation and computational fluid dynamics programs, *Building and Environment* 37 (2002) 857–864.
- [15] FLUENT 6.3 User's Guide, Fluent Inc., Lebanon, USA, 2005.
- [16] Z. Zhang, W. Zhang, Z. Zhai, Q. Chen, Evaluation of various turbulence models in predicting airflow and turbulence in enclosed environments by CFD: part 2-comparison with experimental data from literature, *HVAC&R Research* 13 (6) (2007) 871–886.
- [17] Z. Zhai, Z. Zhang, W. Zhang, Q. Chen, Evaluation of various turbulence models in predicting airflow and turbulence in enclosed environments by CFD: part 1-summary of prevalent turbulence models, *HVAC&R Research* 13 (6) (2007) 853–870.
- [18] P.Y. Chou, On the velocity correlations and the equations of turbulent vorticity fluctuation, *Quarterly of Applied Mathematics* 1 (1945) 33–54.
- [19] A.N. Kolmogorov, Equations of turbulent motion of an incompressible fluid, *Izvestia Academy of Science, USSR, Physics* 6 (1–2) (1942) 56–58.
- [20] P.L. Betts, I.H. Bokhari, Experiments on turbulent natural convection in a enclosed tall cavity, *International Journal of Heat and Fluid Flow* 21 (2000) 675–683.